[1]Shumei Xiao

Optimal Control Strategies for Maximizing Energy Efficiency in Electric Vehicle Charging Infrastructure

JES Journal of Electrical Systems

Abstract: - Among the workable technology alternatives to address the escalating climate change challenges is the transition to electrified transportation. The possibility of shared transport systems and intelligent cars accompany this shift. To move forward and keep comfortable driving conditions, an electric car only uses its stored electric energy. Energy management system (EMS) upgrades are crucial to enhancing efficiency, performance, sustainability of electric vehicles (EVs), as demand for EVs rises steadily. This research propose novel technique in enhancing and maximizing the energy efficiency of electric vehicle based on their charging infrastructure. Here the electric vehicle energy management system has been carried out based on ultracapacitor solar fuel cell and the energy optimization has been carried out using Gaussian grey whale Krill Herd optimization method. Experimental analysis is carried out in terms of energy efficiency, power consumption, Mean Absolute Percentage Error (MAPE), accuracy, robustness. proposed technique attained MAPE of 54%, Accuracy of 97%, ROBUSTNESS of 92%, power consumption of 95%, energy efficiency of 98%. A evaluation based on simulation is carried out, confirming the improved efficiency of the suggested techniques in preserving energy under various driving circumstances.

Keywords: electric vehicle, energy management systems (EMS), charging infrastructure, ultracapacitor, solar fuel cell

1. Introduction:

Energy storage systems, or ESSs, are widely utilised in renewable energy systems, microgrids, and electric vehicles (EVs). Worldwide, the usage of electric vehicles (EVs) has increased significantly since they were considered a suitable replacement for internal combustion engines (ICE). As it stands, ICE vehicles, ships, freight, and aeroplanes have consumed one-third of fossil fuel. In the transportation industry, 94% of vehicles are fueled by oil, 1% use electricity, 2% use biofuel, and 3% use natural gas. According to research, the main emitters of carbon dioxide (CO2), sulphur dioxide (SO2), carbon monoxide (CO), nitrogen oxides—which are main contributors to air pollution and greenhouse gas emissions—are factories and ICE [1]. The ESS in an EV powers the EV motor in addition to additional features like air conditioning and navigation lights. Since EVs emit no CO2, CO2, NO, or SO2 while in motion, they are regarded as zero-carbon vehicles and can help solve environmental issues including the use of fossil fuels [2]. Globally, almost 5 million electric vehicles are listed. In US, EV sales are up 2%, in Portugal, 3%, in China, 7% in Ireland, 8% in Netherlands, 50% of new EVs have been sold in Norway. There were an estimated 450 000 EV travellers in 2015. This was followed by a sharp increase in the market for EVs, with 2.1 million EV passengers in 2019. These days, the market for EV is growing rapidly in China and Europe. On the other hand, the environment that reduces greenhouse gas emissions and global warming by replacing internal combustion engine vehicles with electric vehicles is in danger. Policies encouraging the usage of electric vehicles have been put into place by numerous nations and businesses [3]. These methods make managing and implementing EVs easier and are more futuristic. As of right now, EVs are seen as an achievable energy source that can be delivered over a microgrid or grid and includes coordinated charging attempts to counteract erratic solar and wind power generation. ESS in EVs has amazing power that may scale from 17 kWh to 100 kWh at the moment. Energy management systems provide EVs with future electricity supply during pick-up load period. This makes it possible to connect a renewable electrical infrastructure to grid and enable grid-to-vehicle (G2V) and vehicle-to-grid (V2G) connections. Since charging time accounts for a sizable amount of overall trip time, charging behaviour is significantly influenced by it [4]. Due to the influence of unobservable elements and the climate on EV charging times, it is typically difficult to anticipate charging times with precision. A significant amount of data about EV charging events may be gathered using innovative techniques for data collection. Initial State of Charge (SOC), charging voltage, random arrival and departure times are some of the elements that affect charging time. The charger and EV's

[1] Office of Science and Technology Administration, Yangzhou Polytechnic College, Yangzhou 225009, China

Corresponding Author: Shumei Xiao

E-mail: xiaoshumei1975@163.com

voltage and current limitations, however, determine how long the EV will take to charge. The charger provides current and matches the voltage of the battery when it is first plugged in. Whichever limit is lower, the charger or the EV is limiting this current. More so than the high voltage, the low voltage has a substantial impact on charging time. Data comprise a number of unobservable influencing elements in addition to observable ones. As such, choosing a model that works well and can deal with uncertainty is difficult. A reliable method for obtaining an accurate charging time prediction is to build a model using data. ML-based energy optimisation method for electric vehicles (EVs) is one such solution. It makes predictions about energy use and optimises energy usage by analysing past driving data. By using data from traffic, weather, and driving behaviours, machine learning algorithms may provide drivers with individualised energy management solutions. These solutions can increase the driving range of an EV by reducing energy waste [5].

The major contribution is as follows:

- To propose novel electric vehicle energy maximization with optimization model based on their charging infrastructure analysis.
- To optimize and develop EMS using ultracapacitor solar fuel cell and Gaussian grey whale Krill Herd optimization model
- The energy management system's suggested control system is proven to be successful across a broad range of processes in the electric vehicle application, according to the results. a comparative analysis is made on system design and voltage variations. battery lifetime will be extended and efficiency can be maximized.

2. Background and literature review:

The use of novel techniques to accurately forecast EV energy usage is supported by current research, which also extends driving range as well as lessens range anxiety. Therefore, a larger range can be achieved by empowering drivers to feel more competent as well as allowing them to use car longer on a single charge. In order to provide next stage demand reference to operating efficiency optimisation of ICE, a driving cycle predictor based on MC is built in [6]. Based on anticipated braking torque by MC, stochastic DP (SDP) is utilised in [7] to optimise downshifting control for HEVs during regenerative braking. In [8], near-future driving velocity is predicted using a multi-step Markov prediction method, and the energy flow in PHEVs is subsequently managed by applying the MPC. An offline EMS based on reinforcement learning (RL) is examined in [9] using integrated stationary Markov transition probability matrix. In [10], transportation pattern is identified by using a Markov chain model and using clustering analysis to find characteristic specifications of transportation data. To maximise fuel efficiency of plug-in hybrid electric vehicles (PHEVs), study [11] combined driving condition detection, realised by learning vector quantization neural network, into PMP based energy management. A notable optimisation effect was achieved. The driving cycles were split into three categories by the author [12] using fuzzy C-means clustering, and the condition recognition was finished by calculating distance between value of attributes of actual driving circumstances as well as clustering centre. Machine learning is the primary source of inspiration for recognition techniques. According to NEDC driving cycle, Work [13] separated actual driving conditions into five categories. The BP neural network was then used to recognise the driving conditions, resulting in a high degree of condition identification accuracy. Author [14] investigates how the power grid is affected by the various charging behaviour states, including off-peak, delayed, coordinated/uncoordinated charging. Decentralised EV charging solutions were devised in work [15] to assure charge completion in distribution grid as well as minimise load variance. A multiagent simulation method for spatial distribution of EV ownership among local populations was proposed by author [16]. Using a variety of charging techniques, the effects of charging behaviour associated with growing EV ownership on local power system were examined.

3. EV energy management system using ultracapacitor solar fuel cell (UCSFC):

EV fuel cell power system is composed of a number of parallel fuel cell groupings that work together to produce necessary voltage and current to power electric motor. Fuel cell power method concept for an electric car is depicted in Figure 1. There are two types of loads for EVs: transient and steady. There is no peak demand for a

constant load, such as for on-board electricity or air conditioning. These loads are totally compatible with FC and never fluctuate. Acceleration, braking, and deceleration are all part of the transient load.

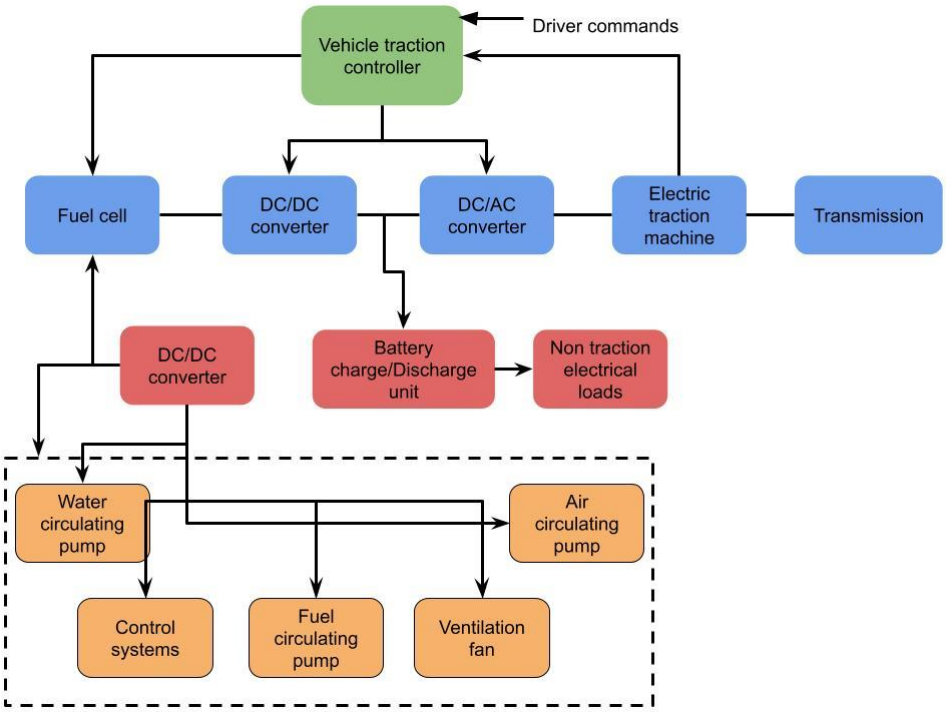

Figure 1. Fuel cell system for EVs

The following formula is utilized to find fuel cell system's global voltage by eqn (1)

$$V_{FC} = N_S(V_r - \Delta V_{act} - \Delta V_{\text{ohm}} - \Delta V_{\text{conc}}) \quad (1)$$

Vr is fuel cell's reversible voltage, ΔV is voltage drop, Ns is number of fuel cells in a serial configuration. The sub-indices act, ohm, and conc take into consideration the effects of mass transit on concentration, ohmic losses resulting from ionic and contact resistance, and the activation process of chemical species. The following mechanism determines how much total current (IFC) a group of fuel cells generates based on the flow of hydrogen by eqn (2)

$$I_{FC} = 2N_p e^{-\frac{\rho_{H_2}\dot{V}_{H_2}}{M_{H_2}}} \quad (2)$$

The fuel cell system's number of parallel cells is denoted by Np, the electron electric charge is represented by e−, and the density, molecular weight, and hydrogen flow are shown by ρH2, MH2, and • VH2, respectively. Equation (3) combined yields the fuel cell power, or PFC:

$$P_{FC} = 2N_sN_p[(V_r - \Delta V_{\text{act}} - \Delta V_{\text{ohm}} - \Delta V_{\text{conc}})]e^{-\frac{\rho_{H_2}\dot{V}_{H_2}}{M_{H_2}}} == 2N_sN_p(V_r - \Delta V)e^{-\frac{\rho_{H_2}\dot{V}_{H_2}}{M_{H_2}}} \quad (3)$$

Taking into account that both the voltage drop, ΔV, and the reversible fuel cell voltage remain constant by eqn (4)

$$P_{FC} = C_{H_2}\dot{V}_{H_2} \quad (4)$$

where constant CH2 is given by eqn (5)

$$C_{H_2} = 2N_5N_p(V_r - \Delta V)e^{-\frac{\rho_{H_2}}{M_{H_2}}} \quad (5)$$

Power is supplied by the UC under temporary load conditions. The model is made up of capacitance Cuc and series equivalent resistance Rsc, which stand for charging and discharging, respectively. The equivalent parallel

resistance, or Rpc, is a representation of self-discharging losses. One way to express the voltage level of UC is given by eqn (6)

$$V_{\mathrm{uc}}(t) = V_{\mathrm{init}}\, e^{\left(-\frac{t}{C_{\mathrm{uc}}R_{\mathrm{sc}}}\right)} \tag{6}$$

The energy extracted from UC can be written as follows is given by eqn (7)

$$E_{\mathrm{uc}} = \frac{1}{2}C_{\mathrm{uc}}(V_{\mathrm{init}}^2 - V_{\mathrm{final}}^2) \tag{7}$$

where Vfinal is the voltage at which the discharge process ends and Vinit is the value at which it begins. Depending on where switch S1 is located, the converter can be in one of two states. When a signal is applied at the gate to turn on switch S1, the diode will not conduct, the inductor current will equal the source current, and the switch will conduct the same current. At this time, the output capacitor Cout will be the only source of load current, and the inductor will be storing energy. When switch S1 is turned off, the diode will become forward-biased and the inductor current will pass through it, charging the capacitor that was discharged during the preceding situation. The car can only be driven by the electric accumulator, regardless of the driving conditions. When the battery encounters an excessive discharge rate during periods of high power consumption, such as during the acceleration process or in areas with a slope, this results in a decreased battery capacity and a shorter driving range. Because the fuel cells function poorly at high discharge rates, which happen during the acceleration phase, fuel cell-powered electric cars have difficult acceleration. Fuel cell manufacturers expanded their product lines to circumvent this issue and supply the electric car with adequate power during periods of high power consumption. Hybrid fuel cell and supercapacitor systems circumvent the problems of rapid discharge and inability to tolerate high discharge rates. Actually, the electric automobile is powered by supercapacitor during periods of high power demand, fuel cell operates at medium or low power demand. The supercapacitor is also recharged by the fuel cell after use, but the discharge rate is far lower because the supercapacitor recharges more slowly than discharge.

Because ultracapacitors have a cell voltage of 2.7 V, using them as energy storage devices in hybrid electric vehicles (HEVs) requires connecting multiple cells in series to achieve a high voltage level. Fuel cell's as well as supercapacitor's physical characteristics were taken into consideration when developing the power distribution plan. Because of its high energy density, fuel cell is intended to be used as main energy source majority of time. Due to its low power density, the fuel cell can operate continuously in low-load, stable settings. However, the high power density of the supercapacitor makes it perfect for high transient load scenarios. Because supercapacitor discharges quickly and offers significant power to the vehicle, it is employed as a secondary energy source due to its low energy density. The following is an overview of power management strategy:

1. Majority of fuel cell's operation occurs at low power requirements. The supercapacitor is charged with the leftover energy. Supercapacitors are charged and discharged in accordance with the demands of the load.
2. To satisfy high power requirements, fuel cell is temporarily powered by supercapacitor during high power demands.

Nonlinear controllers were used to implement the previously outlined technique, and the outcomes are shown. This approach was chosen because it: (1) uses nonlinear controllers to distribute power in real-time for speed control; (2) does not require prior knowledge of driving cycle; (3) considers properties of both fuel cell as well as supercapacitor when distributing power; and (4) is easily implemented online. Neural networks, artificial intelligence, and optimization-based techniques can be applied to ensure the best possible HESS performance; however, these techniques have three drawbacks: (1) they require a lot of computational power; (2) they operate offline; and (3) they overlook real-world vehicle power requirements, like power needed to accelerate in presence of gravity as well as friction. (4) are difficult to execute. The controller equations for adaptive controllers based on Lyapunov as well as backstepping will be officially derived in the following stage. We create an adaptive parametric update rule for unknown time-varying specifications after first assuming that all of the parameters are known.

4. Energy optimization using Gaussian grey whale Krill Herd optimization model (GGWKHO):

To increase forecasting accuracy, the GP model makes use of data from several sources (tasks); from now on, sources and tasks is utilized interchangeably. By transferring important information between tasks and extracting and learning the commonalities between them, forecasting accuracy is improved. It should be highlighted that task similarities are solely derived from observations of individual tasks; they are taught by inter-task dependency. Utilising a parameterized covariance function over input variables, this inter-task dependency matrix is used. Assume that there are N different inputs (x1, x2, • • •, xN) for each of the Z tasks. The energy consumption in this study, which is response variable, can thus be expressed as follows by eqn (8)

$$\boldsymbol{y} = (y_{11}, \cdots, y_{1N}, y_{12}, \cdots, y_{N2}, \cdots, y_{1Z}, \cdots, y_{NZ}) \tag{8}$$

where yil denotes the result of lth task and xi the ith input. We assume a GP prior with zero mean over latent functions fl to solve this issue. As a result, relationships between tasks can be shown as follows by eqn (9)

$$\langle f_l(x) f_k(x') \rangle = K_{lk}^f k^x(x, x'),\ y_{il} \sim N(f_l(x_i), \sigma_l^2), \tag{9}$$

Furthermore, for the l th job, the noise variance is σ 2 l. It is assumed that k x is a stationary covariance function in this model. Joint Gaussian distribution over y is taken to be non-block-diagonal. Matrix's off-diagonal members take non-zero values because it isn't a block-diagonal matrix in relation to jobs. Due to this characteristic, predictions and observations from one job might have an impact on observations from other tasks. Therefore, it can be verified that tasks are transferring significant information. Additionally, by understanding the covariance function given in (2), predictive distribution may be determined by applying conventional Gaussian Process equations for mean as well as variance. Consequently, mean and covariance for a fresh set of data x in task l can be expressed as follows by eqn (10)

$$\begin{aligned} \bar{f}_l &= \left(k_l^f \otimes k_*^x\right)^T \Sigma^{-1} \boldsymbol{y}, \\ \Sigma &= k^f \otimes k^x + D \otimes I, \end{aligned} \tag{10}$$

Fundamental concept of GWO is quite similar to the hunting strategy and leadership structure of wolves. Generally speaking, four distinct wolf types—alpha (α), beta (β), delta (δ), and omega (ω) wolves—are simulated, arranged in order of strength. The first three sorts of wolves working together to seek the prey and arrive at a better solution are represented by the best three solutions in order to locate a new one. GWO simulates social hierarchy, tracking, surrounding, and attacking behaviours of a grey wolf statistically by eqn (11)

$$\begin{aligned} \vec{D} &= \left| C \cdot \vec{X}_p(t) - \vec{X}(t) \right| \\ \vec{X}(t+1) &= \vec{X}_p(t) - A \cdot \vec{D} \\ A &= 2ar_1 - a \\ C &= 2r_2 \\ a &= 2 - \mathrm{t}\frac{2}{\mathrm{Max\_iter}} \end{aligned} \tag{11}$$

where an is a linearly declining coefficient from 2 to 0, Max_iter is maximum number of iterations, and $r1$ and $r2$ are equally distributed random values, 0 and 1. When hunting, alpha wolves (α) take the lead over the other wolves. In addition, beta (β) and delta (δ) wolves engage in hunting activities. In every iteration, the optimal solutions from alpha (α), beta (β), and delta (δ) are preserved, remaining omega (ω) wolves adjust their placements in response to them. The following equations are suggested in this regard by eqn (12)

$$\begin{aligned} \vec{D}_\alpha &= \left| C_1 \cdot \vec{X}_\alpha - \vec{X} \right| \\ \vec{D}_\beta &= \left| C_2 \cdot \vec{X}_\beta - \vec{X} \right| \\ \vec{D}_\delta &= \left| C_3 \cdot \vec{X}_\delta - \vec{X} \right| \end{aligned} \tag{12}$$

where position vectors for alpha (α), beta (β), delta (δ) , $X\ \alpha$, $X\ \beta$, and $X\ \delta$. The vectors $C1$, $C2$, and $C3$ are produced randomly, whereas X is position vector of individual in question. Distance between current individual location and that of individual alpha (α), beta (β), and delta (δ) is measured by equations (13). Thus, the present individual's final position vectors are found by:

$$\vec{X}_1 = \vec{X}_\alpha - A_1 \cdot \vec{D}_\alpha$$
$$\vec{X}_2 = \vec{X}_\beta - A_2 \cdot \vec{D}_\beta$$
$$\vec{X}_3 = \vec{X}_\delta - A_3 \cdot \vec{D}_\delta \quad (13)$$

where the vectors $A1$, $A2$, and $A3$ are produced at random. A new position (solution) is created by combining the three best positions by eqn (14)

$$\vec{X}(t+1) = \frac{w\bar{X}_1 + w\bar{X}_2 + w\bar{X}_3}{3} \quad (14)$$

Three steps make up the WOA process: bubble assault (local search), prey encircling (global search), and prey searching (iterate updating). Updating each whale's location is the aim of prey seeking. Prey encirclement serves the objective of allowing individual whales to finish their worldwide search for ideal targets. The goal of the bubble assault is to achieve local optimisation. The number of whales in the population should first be initialised, and the number of iterations should be optimised. Assume that N is size of the whale population, D is optimised parameter dimension, and M is the optimal number of iterations. Every whale location in WOA stands for a potential fix for the optimisation issue. Let i be the number of distinct whales. If i = 1, 2,..., N, then position of i-th individual in the whale population is Xi = (x1 i, x2 i,..., xD i). Furthermore, the global optimal solution is whale at ideal preying position. Fuel consumption of vehicle is the fitness value f (x), which may be expressed as follows by eqn (15)

$$f(x) = \sum_{f=1}^{N} \left(b_{\text{cor}}(X) + \omega_t \frac{P_{\text{har}}(X)}{Q_{\text{lir}}} \right) \quad (15)$$

When t is time step, ωt is energy consumption conversion rate, Qlhv is fuel low heat value. To guarantee that various components can work within tolerances, certain powertrain performance as well as vehicle dynamic limitations are specified throughout the optimisation process. Set up each Krill individual: Provide a starting population of krill individuals, each represented by the GRP parameters C and σ and given a position in the search space as Ki. Set their starting points at random points in the search space by eqn (16)

$$\theta_i, \phi_i \in [\theta_{\min}, \theta_{\max}] \times [C_{\min}, C_{\max}] \times [\sigma_{\min}, \sigma_{\max}] \quad (16)$$

Krill Movement: Movement of Separation: Krill people usually keep a minimum gap between themselves. Using the separation factor as a basis, compute the new position by eqn (17)

$$\theta_i(t+1) = \theta_i(t) + \Delta\theta_i(t+1) \quad (17)$$

Where

$$\Delta\theta_i(t+1) = \Delta s \sum_{j=1}^{N} d\big(\theta_i(t), \theta_j(t)\big)\big(\theta_i(t) - \theta_j(t)\big)$$

Alignment Movement: Krill modify their velocities to match those of their neighbours. Determine the alignment factor and use it to calculate the new position by eqn (18)

$$\theta_i(t+1) = \theta_i(t) + \Delta\theta_i(t+1)$$
$$\Delta\theta_i(t+1) = \Delta a \sum_{j=1}^{N} \big(\phi_j(t) - \phi_i(t)\big)\big(\theta_j(t) - \theta_i(t)\big) \quad (18)$$

For Krill Herd Algorithm (KHA) to produce accurate predictions and efficient optimisation, parameter values must be chosen carefully. Parameter decisions like separation (¬s), alignment (¬a), cohesiveness (¬c), attraction (¬f), and distraction (¬e) variables are crucial for striking this balance between exploration and exploitation. Exploiting potential regions and conducting sufficient investigation of the solution space are ensured by prioritising values that support both exploration as well as exploitation. This promotes convergence towards the global optimum and delays the premature convergence to suboptimal solutions. In addition, parameter values are customised based on the features of the data, including its size, variability, and complexity. To highlight

exploiting and refining solutions effectively, for instance, larger numbers are preferable in settings with well-defined patterns or abundant data, whereas smaller values may be chosen in situations with significant variability or scant data to encourage additional exploration.

5. Experimental analysis:

The simulation operates on a 2.5 GHz personal computer outfitted with an Intel Core i5 processor, 8 GB of RAM, and RAM, using the Simulink version of MATLAB-2017. Initially, VFT is connected to a doubly-fed, 3-phase, asynchronous machine with a rated speed of 1500 rpm, 15.1 kVA, 400 V, and 50 Hz. A three-phase series R-load is then connected. By means of its stator windings, a DC motor isolates R-Load linked to WRIM and modifies the SG speed. In this section, we perform simulations to illustrate the relationships between the average EV arrival, average cost, average cost upper bound, and average EV queue duration. We consider different capacities and numbers of charge points of the battery used for renewable energy storage in interim. In the simulations, "energy block" has a size of E = 10 and a period length of 1. In simulations, we employ radical policy. For A, Ea, and P, we consider i.i.d. cases. The probability of A taking 0 and 2A is equal. With the probability of 1, 0, and 0, EA accepts the numbers 0, 50, and 100. With the probability of 0, 2, and 0.5, P accepts the numbers 5, 10, and 20. Performance has been averaged across 105 periods. M = 50 and M = 8 are the numbers of charge sites that we have set. Plotted are the curves for various storage battery capacities, including Emax = 100, Emax = 300, and limitless capacity. But when A is large (say, A 10), cost increases quickly as A increases, essentially following a linear relationship. This is such that when A is tiny, the battery can supply energy and the necessary energy is equally little. Consequently, there won't be any costs and no consumption of grid power. When A surpasses a predetermined threshold and the needed energy exceeds energy in batteries, grid power is used. Since M is huge, we have k = minq, M = q with a high probability, meaning that the performance will not be impacted by the constraint on the number of charge sites. The power consumption on grid will rise in tandem with an increase in A. Moreover, grid power takes over as the primary energy source when A is high. We conclude from (5) that there is roughly a linear link between the cost and A. Power consumption is evaluated using equation (3), where br and θr are set to 137 mW/Mbps and 132.9 mW, 52 mW/Mbps, 1288 mW for LTE and WIFI. After path r's energy consumption is equal to product of Pr and during T, we can calculate the machinery's total energy consumption by adding energy consumption of each interface.

Table-1 Comparative based on EV charging power range

Cases	Techniques	MAPE	Accuracy	Robustness	Power consumption	Energy efficiency
137 mW/Mbps and 132.9 mW	**ELM**	78	74	73	75	79
	PSWO	73	76	78	79	83
	UCSFC_GGWKHO	70	88	80	84	89
52 mW/Mbps and 1288 mW	**ELM**	79	85	81	83	92
	PSWO	62	89	87	90	95
	UCSFC_GGWKHO	54	97	92	95	98

Table-1 shows comparative for EV charging power ranges. the proposed technique analysed based on 137 mW/Mbps and 132.9 mW, 52 mW/Mbps, 1288 mW in terms of MAPE, Accuracy, Robustness, power consumption, energy efficiency.

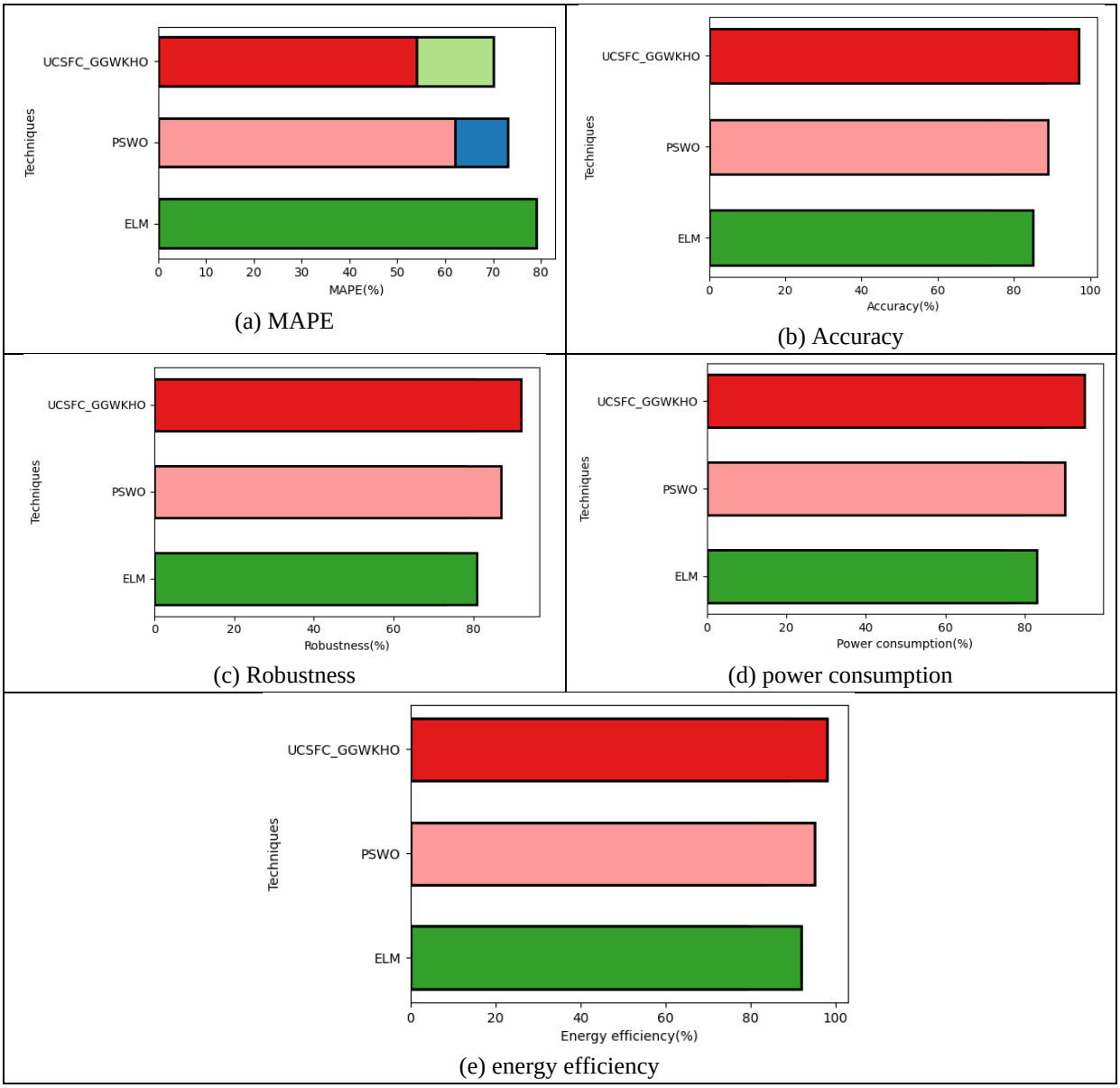

Figure-3 Comparative for 137 mW/Mbps and 132.9 mW in terms of (a) MAPE, (b) Accuracy, (c) ROBUSTNESS, (d) power consumption, (e) energy efficiency.

Figure- 3 shows comparative for137 mW/Mbps and 132.9 mW. proposed technique attained MAPE of 70%, Accuracy of 88%, ROBUSTNESS of 80%, power consumption of 84%, energy efficiency of 89%, ELM attained MAPE of 78%, Accuracy of 74%, Robustness of 73%, power consumption of 75%, energy efficiency of 79%, PSWO attained MAPE of 73%, Accuracy of 76%, Robustness of 78%, power consumption of 79%, energy efficiency of 83%. for 52 mW/Mbps and 1288 mW proposed technique attained MAPE of 54%, Accuracy of 97%, Robustness of 92%, power consumption of 95%, energy efficiency of 98%, ELM attained MAPE of 79%, Accuracy of 85%, Robustness of 81%, power consumption of 83%, energy efficiency of 92%, PSWO attained MAPE of 62%, Accuracy of 89%, Robustness of 87%, power consumption of 90%, energy efficiency of 95%.

Simplifying the method is siginificant in order to lessen the computational load of DP. The power output of EM is control variable, while energy stored in battery is dynamic state. Backward DP algorithm assesses cost of each permitted torque split at a specific time instant and uses kinematical equations to compute the power demanded by driver based on vehicle velocity. Ultimately, trajectory that minimises fuel consumption from initial to the ultimate state of charge yields optimal solution, or series of power values that EM must supply. Due to discretization of state variable, which is set between SOCmin = 0.6 and SOCmax = 0.8, SOC requirement is automatically satisfied. Accurate power demand data is difficult to come by because vehicle movement is

influenced by a number of variables, including traffic and driving habits. Formulates an immediate optimisation problem for a battery-UC HESS power split problem in order to solve an EM problem without future operating knowledge available. To make the best use of the UC, it must be charged or discharged appropriately. Given the difficulty in predicting future power consumption profiles, the UC SoC can be adjusted with a straightforward method depending on vehicle speed (Vs): In order for UC to produce stored energy that can meet peak power during accelerations, it is recommended that UC be run in a high SoC range whenever Vs is low. In contrast, due of regenerative power during decelerations, the UC SoC must be low if Vs is high. Specifically, whenever the Vs rises from zero, the electric machine often needs a lot of power.

6. Conclusion:

Based on the infrastructure for charging electric vehicles, this study offers a revolutionary method for optimising and increasing energy efficiency. The energy management system for this EV is based on an ultracapacitor solar fuel cell, and the Gaussian grey whale Krill Herd optimisation model was used to optimise the energy use. Fuel consumption is somewhat reduced at fixed state discretization when action discretization is increased, but the benefit is negligible above a certain point. Conversely, fuel consumption increases with increasing state discretization at the fixed action discretization. However, after a certain discretization threshold, the rate of fuel consumption increase becomes negligible. The MPG increases to a certain point and then starts to decline when both states and action discretization increase simultaneously. Following the classification of a particular traffic state, the ideal control levels for various driving situations will be called online. Finally, a simulation-based evaluation is carried out to confirm the improved energy-saving performance of the suggested solutions under various driving scenarios. Future iterations of the model will account for other factors like traffic circumstances, driver behaviour, and auxiliary loads. Examining the effectiveness of sophisticated deep learning methods and rigorous optimisation would also be beneficial.

Funding :

This work is funded by the Soft Science Research Project of the Special Innovation Support Program of Jiangsu Science and Technology Plan in 2023 (BR2023020-4).

Reference:

[1] Karmaker, A. K., Hossain, M. A., Pota, H. R., Onen, A., & Jung, J. (2023). Energy management system for hybrid renewable energy-based electric vehicle charging station. *IEEE Access*, *11*, 27793-27805.

[2] Manivannan, R. (2024). Research on IoT-based hybrid electrical vehicles energy management systems using machine learning-based algorithm. *Sustainable Computing: Informatics and Systems*, *41*, 100943.

[3] Huy, T. H. B., Dinh, H. T., Vo, D. N., & Kim, D. (2023). Real-time energy scheduling for home energy management systems with an energy storage system and electric vehicle based on a supervised-learning-based strategy. *Energy Conversion and Management*, *292*, 117340.

[4] Candan, A. K., Boynuegri, A. R., & Onat, N. (2023). Home energy management system for enhancing grid resiliency in post-disaster recovery period using Electric Vehicle. *Sustainable Energy, Grids and Networks*, *34*, 101015.

[5] Ye, Y., Zhang, J., Pilla, S., Rao, A. M., & Xu, B. (2023). Application of a new type of lithium-sulfur battery and reinforcement learning in plug-in hybrid electric vehicle energy management. *Journal of Energy Storage*, *59*, 106546.

[6] Huy, T. H. B., Dinh, H. T., & Kim, D. (2023). Multi-objective framework for a home energy management system with the integration of solar energy and an electric vehicle using an augmented ε-constraint method and lexicographic optimization. *Sustainable Cities and Society*, *88*, 104289.

[7] Louback, E., Biswas, A., Machado, F., & Emadi, A. (2024). A review of the design process of energy management systems for dual-motor battery electric vehicles. *Renewable and Sustainable Energy Reviews*, *193*, 114293.

[8] Jondhle, H., Nandgaonkar, A. B., Nalbalwar, S., & Jondhle, S. (2023). An artificial intelligence and improved optimization-based energy management system of battery-fuel cell-ultracapacitor in hybrid electric vehicles. *Journal of Energy Storage*, *74*, 109079.

[9] Saravanan, R., Sobhana, O., Lakshmanan, M., & Arulkumar, P. (2023). Fuel cell electric vehicles equipped with energy storage system for energy management: A hybrid JS-RSA approach. *Journal of Energy Storage*, *72*, 108646.

[10] Zhang, H., Peng, J., Dong, H., Tan, H., & Ding, F. (2023). Hierarchical reinforcement learning based energy management strategy of plug-in hybrid electric vehicle for ecological car-following process. *Applied Energy*, *333*, 120599.

[11] Belkhier, Y., Oubelaid, A., & Shaw, R. N. (2024). Hybrid power management and control of fuel cells-battery energy storage system in hybrid electric vehicle under three different modes. *Energy Storage*, *6*(1), e511.

[12] Chatterjee, D., Biswas, P. K., Sain, C., Roy, A., & Ahmad, F. (2023). Efficient energy management strategy for fuel cell hybrid electric vehicles using classifier fusion technique. *IEEE Access*.

[13] Huang, Y., Hu, H., Tan, J., Lu, C., & Xuan, D. (2023). Deep reinforcement learning based energy management strategy for range extend fuel cell hybrid electric vehicle. *Energy Conversion and Management*, *277*, 116678.

[14] Yu, X., Lin, C., Tian, Y., Zhao, M., Liu, H., Xie, P., & Zhang, J. (2023). Real-time and hierarchical energy management-control framework for electric vehicles with dual-motor powertrain system. *Energy*, *272*, 127112.

[15] Wang, Z., He, H., Peng, J., Chen, W., Wu, C., Fan, Y., & Zhou, J. (2023). A comparative study of deep reinforcement learning based energy management strategy for hybrid electric vehicle. *Energy Conversion and Management*, *293*, 117442.

[16] Zhang, Z., Zhang, T., Hong, J., Zhang, H., & Yang, J. (2023). Energy management strategy of a novel parallel electric-hydraulic hybrid electric vehicle based on deep reinforcement learning and entropy evaluation. *Journal of Cleaner Production*, *403*, 136800.